C72184A

Conf-911001--16

To be Presented at The International Conference on Fast Reactors and Related Fuel Cycles, Kyoto, Japan October 28 - November 1, 1991

Improvements in EBR-II Core Depletion Calculations

ANL/CP--72184

DE91 018646

P. J. Finck, R. N. Hill, and S. Sakamoto*
Reactor Analysis Division

Argonne National Laboratory
9700 South Cass Avenue
Argonne, IL 60439
(708) 972-7063

*Permanent Address: Reactor Research Institute, Kyoto University

* Work supported by the U.S. Department of Energy, Nuclear Energy Programs under Contract W-31-109-ENG-38.

Improvements in EBR-II Core Depletion Calculations

P. J. Finck, R.N. Hill, and S. Sakamoto*
Reactor Analysis Division
Argonne National Laboratory
Argonne, IL 60439-4801, USA

ABSTRACT

The need for accurate core depletion calculations in Experimental Breeder Reactor No. 2 (EBR-II) is discussed. Because of the unique physics characteristics of EBR-II, it is difficult to obtain accurate and computationally efficient multigroup flux predictions. This paper describes the effect of various conventional and higher order schemes for group constant generation and for flux computations; results indicate that higher-order methods are required, particularly in the outer regions (i.e. the radial blanket). A methodology based on Nodal Equivalence Theory (N.E.T.) is developed which allows retention of the accuracy of a higher order solution with the computational efficiency of a few group nodal diffusion solution.The application of this methodology to three-dimensional EBR-II flux predictions is demonstrated; this improved methodology allows accurate core depletion calculations at reasonable cost.

1. INTRODUCTION

Experimental Breeder Reactor No. 2 (EBR-II) and its adjoining fuel cycle facility were originally designed and operated to provide a small plant demonstration of a sodium-cooled fast breeder power plant with an integral fuel cycle. Following successful demonstration of the plant, EBR-II has been utilized for many fast neutron irradiation and materials testing experiments. Meanwhile, significant improvements have been developed for metal fuel reprocessing; various process changes, including the use of electrorefining, have reduced the heavy metal losses from 5-10% to less than 1% and virtually eliminated the noble metals from the heavy metal product. This new reprocessing technique is the basis for the Integral Fast Reactor (IFR) fuel cycle concept. Thus, a key milestone of the IFR program is to demonstrate closure of the IFR fuel cycle at EBR-II.

Efficient operation of this closed fuel cycle requires an accurate tracking of all materials during both in-core and ex-core phases. It is particularly important to trace actinide isotopes, since fissile material recovery is the purpose of reprocessing. Chemical and isotopic analyses of the discharged fuel is impractical on a large scale. Therefore, accurate core depletion calculations are necessary to specify the material composition of the spent and reprocessed fuel.

The EBR-II system has unique physics characteristics which make it difficult to generate accurate multigroup neutronic solutions; these characteristics are discussed in Section II. The generation of group constants for EBR-II flux predictions is addressed in Section III; and the weaknesses of standard (i.e. diffusion theory) calculational methods are evaluated in Section IV. Methodological improvements and their implementation in the DIF3D nodal diffusion theory code are discussed in Section V. Practical applications to EBR-II core calculations are demonstrated in Section VI.

* Permanent Address: Reactor Research Institute, Kyoto University

2. PHYSICS CHARACTERISTICS OF EBR-II

EBR-II is a small core with a power rating of 62.5 MWt. The core height is ~35 cm with a radius of 30-35 cm; thus, the H/D ratio is ~1/2 indicating a pancaked core geometry. Both the small core size and geometric spoiling lead to a high neutron leakage fraction; about 60% of the neutrons produced leak out of the core.The high neutron leakage fraction leads to the large discrepancies between diffusion and transport theory, as discussed in Section IV.

The ex-core configuration of EBR-II creates additional physics complications. First, in the axial direction there is a plenum region above the core and a reflector below the core (note that the pancaked design makes axial leakage dominant in the core). This leads to an axial power tilt toward the lower part of the core. The severity of this tilt depends upon the relative magnitudes of upper and lower leakage; these leakage rates are strongly influenced by:

1., the significant streaming path within the pin in the upper plenum leading to inaccuracies when a homogenized treatment is used.

2. , the significant reflection back into the core from the lower reflector; this requires an accurate modeling of neutron scattering anisotropy. This modeling is further complicated by the dominance of resonance scattering in the steel reflector.

The radial configuration of EBR-II is particularly unique; the radial reflector is adjacent to the core and is surrounded by several rows (~45 cm thick) of radial blanket. Flux predictions in the radial blanket are of particular importance since technical specifications limit the coolant outlet temperature and since radial blanket lifetime is limited by fluence[1].However, physics predictions in radial transition zones are especially difficult. As discussed in Ref. 2, discrepancies between predictions and experiments increase with penetration in a uniform blanket zone; in Ref. 3, these errors are attributed to directional dependancy of the transitional resonance spectra and group constants. Similar effects are caused by the iron resonances within the radial reflector; these phenomena are particularly important when accurate modeling of the neutron reflection back into the core is required. Many of the important iron resonances can be accurately modeled by refining the energy group structure. However, the narrow iron resonances and most high energy actinide resonances cannot be represented by multiple energy meshes in any practical group structure.

3. ANALYSIS OF GROUP CONSTANT GENERATION

As discussed above, accurate modeling of the reflection of neutrons in EBR-II may require refinements of the neutron energy group structure; because of the high leakage fraction, the core multiplication factor is particularly sensitive to the reflection rate. In addition, the radial and axial flux distributions require an accurate modeling of the neutron transmission and reflection. To assess the importance of group structure, eigenvalue calculations for a wide variation of energy group distributions have been compared.

For this analysis, fine group neutron cross sections are generated using the MC2-2 code[4]. In MC2-2, an infinite medium spectrum is calculated for a 2082 energy group structure with resonance reaction rates calculated separately; group constants are then generated by condensation to the specified group structure. Fine group constants were generated for three compositions (representative of the core, radial reflector, and radial blanket) in a 230 group energy structure. The infinite medium calculation for the core composition utilized a buckling search to criticality whereas the reflector and blanket calcula-

tions utilized a fixed source proportional to the incoming leakage source in each region. Using the transport theory code TWODANT[5], the flux distribution (S8P1) was calculated for a simplified R-Z model of EBR-II. The fine energy group constants were then collapsed over several spatial zones to various broad group structures using the fine group flux solution.

In Table I, the computed eigenvalues for the various group constant sets are compared to a continuous energy Monte Carlo solution (generated using the VIM[6] code); the VIM and MC2-2 cross sections are both generated from identical ENDF/B-V data. As shown in Table I, the eigenvalue varies by 1% between the 9 group and 230 group solutions; the difference decreases to 0.2% if 68 energy groups are used. However, the 230 group solution is 0.9% higher than the continuous energy VIM solution. Use of a more detailed group structure was also analyzed.; for a 274 energy group structure with particular detail in the iron resonances, the eigenvalue is 0.4% lower than the 230 group solution.

TABLE I. EIGENVALUE COMPARISON FOR SIMPLIFIED EBR-II R-Z MODEL (S8P1)

No. of Groups	Keff
9	1.234
21	1.230
50	1.228
68	1.226
230	1.224
274	1.220
274*	1.217
continuous energy	1.215

*with self-shielding of high energy iron cross sections

Several additional refinements to the group constant generation method were also investigated. Because of the "resonance-like" structure of the iron scattering cross section above the resolved resonance range, important self-shielding effects may be neglected in the conventional 2082 energy group MC2-2 library. Using the 274 energy group structure and a self-shielding treatment of the high-energy iron cross section, the eigenvalue decreases by 0.3% as shown in Table I; this group constant set appears to give the closest agreement with the continuous energy solutions. Consistent P1 and B1 collapsing schemes were also investigated; the two generation methods lead to significant differences in the transport cross sections, but it was found that transport theory predictions of the eigenvalue and flux shapess are nearly identical for the two methods.

In summary, accurate prediction of the eigenvalue requires a fine energy group structure with a detailed treatment of self-shielding effects in iron. However, this degree of detail is not practical for depletion applications where large numbers of full core flux calculations are required. Thus, a method has been developed which allows for systematic condensation of fine-group cross-sections into few-group cross-sections while retaining computational accuracy.

4. ANALYSIS OF FLUX COMPUTATION METHODS

Given a set of multigroup cross sections, various methods can be used to compute the flux distribution. Because of the high neutron leakage fraction in EBR-II, large discrepancies between diffusion and transport theory calculations are expected. Since diffusion theory tends to overpredict the neutron leakage, large underpredictions of the eigenvalue and significant errors in the radial and axial flux profiles can be expected.

The accuracy of diffusion theory and various discrete ordinates transport theory approximations were compared. Using nine group cross sections, neutron flux calculations for an idealized R-Z model of the EBR-II core were performed using the DIF3D[7] diffusion theory code and the TWODANT transport theory code. The eigenvalue predictions are compared in Table II. Each calculation utilized a mesh size of 2-3cm; spatial convergence was verified for the S8 solution. As expected, the transport eigenvalue is significantly (4.8%) higher than the diffusion eigenvalue; the transport effects are thus very significant for the small EBR-II core.

TABLE II. EIGENVALUE COMPARISON FOR SIMPLIFIED EBR-II R-Z MODEL

Flux Methodology	Keff
Diff. - P1	0.953
Diff.-B1	0.964
S4P0	1.089
S4P0*	0.990
S4P1	1.004
S8P1	1.002
S16P1	1.001

The anisotropic scattering treatment is also observed to be crucial. The S4P0 transport eigenvalue is about 9% too high, and the transport-corrected S4P0 eigenvalue is 1.4% below the S4P1 solution. Preliminary results indicate that higher order Legendre expansions (P3) of the scattering cross sections may be necessary. Furthermore, the errors attributable to the treatment of anisotropic scattering are expected to depend on the group structure. Low levels of angular quadrature appear to be sufficient: the S4P1 eigenvalue is only 0.3% too high, and the S8P1 value is within 0.1% of the S16P1 result. Work is underway to assess these errors for the fine energy structures which are needed for EBR-II core calculations.

Significant variations in the flux distributions were also observed. The diffusion and transport results agree well (within 2% for the total flux) in the core. However, significant deviations (up to 30%) were observed in the radial blanket. The transport-corrected S4P0 solution also exhibited significant errors in calculated flux distribution; the computed fluxes were 5% too low in the radial reflector and 5% too high in the radial blanket, when compared to the S16P1 solution.

Thus, transport theory calculations with adequate treatment of anisotropic neutron scattering appear to be required for accurate prediction of core neutronics parameters. Unfortunately, the performance of

3-D transport calculations in hex-z geometry is too costly for routine applications; diffusion theory calculations are significantly more efficient, and are very desirable for practical applications where large numbers of such calculations are needed. Thus, a method has been developed, which allows standard full core nodal diffusion calculations to reproduce the results of higher order transport calculations.

5. NODAL EQUIVALENCE THEORY IN HEXAGONAL GEOMETRY

In the previous sections of this paper, results were presented which indicated the need to develop a neutronic methodology which has the computational efficiency of few-group diffusion theory codes, while retaining the accuracy of fine group higher order transport schemes. A promising approach consists of using few group nodal diffusion theory codes, along with "nodal equivalence theory parameters" to preserve some information provided by higher order calculations. This approach is usually known as Nodal Equivalence Theory (N.E.T.). Nodal Equivalence Theory is now routinely and very successfully used for the analysis of light water reactors[8]. Its implementation into modern nodal codes[9], and the development of accurate strategies for approximating the N.E.T. parameters[8] have permitted the creation of very efficient analysis schemes. However, N.E.T. has usually been implemented for cartesian geometry codes and most approximate methods for computing the N.E.T. parameters have been devised for cartesian geometries and thermal systems. Thus, these methods could not be directly applied to the analysis of systems with hexagonal assemblies and fast neutron energy spectra. .

The basic idea which underlies N.E.T. consists of providing the standard diffusion theory equations with additional degrees of freedom (the so called "discontinuity factors") which, when chosen adequately, force the solution of the modified equation to reproduce any previously known higher order solution. To be useful practically, approximate methods must be devised to obtain discontinuity factors which force the solution of the modified equation to be a good approximation to an unknown higher order solution. This approach has been successfully applied to LWR analysis, where errors incurred during spatial homogenization and energy condensation procedures can be reduced by use of discontinuity factors obtained from local (assembly or multi-assembly) approximations of a detailed transport solution.

In this section, we outline the implementation of N.E.T. within the DIF3D [11] nodal hexagonal scheme. The practical application of N.E.T. for EBR-II computations is described in in Section VI..

The following derivations apply to the 3-D hexagonal-Z case - reduction to the 2-D hexagonal geometry case is straighforward. Let subscript s, s=1,2,...,8 enumerate the 8 surfaces (Fig. 1) of each hex-Z node. Let $\alpha \in \{x, u, v, -x, -u, -v, z, -z\}$ denote the 8 respective surface normals of surfaces with coordinates $\pm h/2$ or $\pm(\Delta z)/2$ along α. Subscripts α and s will also enumerate the four flux moment directions $\alpha \in \{x, u, v, z\}$ with s=1,2,3,4 respectively.

For each node and energy group, the nodal variables are (space and energy subscripts are omitted): the node average flux $\bar{\bar{\phi}}$, eight each of the following surface averaged quantities - the flux $\bar{\phi}_\alpha$, the net currents $\bar{J}_\alpha$, the out-going (incoming) partial currents $\bar{J}^o_\alpha$ and $\bar{J}^i_\alpha$, and the 4 directional flux moments M_α. $\vec{J}^o$ and $\vec{J}^i$ are vectors of the eight surface quantities, $\bar{J}^o_\alpha$ and $\bar{J}^i_\alpha$.

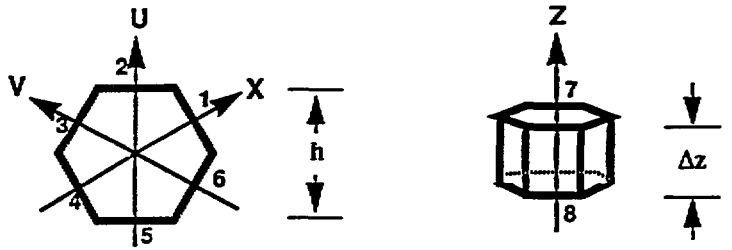

Figure 1: Hexagonal-Z Node Surface Numbering

The nodal variables obey the following equations:[4]

Nodal Balance Equation: $\Sigma^r \bar{\phi} + \bar{L} = \bar{Q}$ (1)

(Σ^r = removal cross section, $\bar{L}$ = leakage term, $\bar{Q}$ = fission and scattering source)

Moment Equation:: $[\Sigma^r + \Sigma^{geo}] M_\alpha = Q_\alpha + \bar{T} + a_\alpha \qquad \alpha = \{x,u,v,z\}$ (2)

(Σ^{geo} = geometrical removal term, which depends on cross-sections and geometrical information, Q_α = directional source moment, $\bar{T}$ = linear combination of net surface currents, a_α = expansion term, which depends on surface fluxes).

Response Matrix Equation: $\tau_1 \bar{\phi}_\alpha + \tau_2 \bar{\phi}_{-\alpha} = F_\alpha^+ \left(\bar{J}^i, \bar{J}^o, \bar{Q}, Q_\alpha \right) \qquad \alpha = \{x, u, v, z\}$ (3)

(τ_1 and τ_2 are geometry dependent, $\bar{\phi}_\alpha$ and $\bar{\phi}_{-\alpha}$ are the surface average fluxes on the right and left sides relative to direction α, F_α^+ is a function of partial currents, sources, geometry, and source moments Q_α with $Q_{-\alpha} = Q_\alpha$).

Surface fluxes are eliminated in favor of surface partial currents by making use of

$$\phi_\alpha = 2 (J_\alpha^o + J_\alpha^i) \tag{4}$$

Interface Continuity Relations: $\bar{J}_\alpha^{o,k} = \bar{J}_{-\alpha}^{i,k'}$ and $\bar{\phi}_\alpha^k = \bar{\phi}_{-\alpha}^{k'}$ (5)

(node k' is the neighbor of node k in direction α)

Let us assume that some neutronic solution (called from now on "reference" solution) of the core is known. The known reference quantities are $\bar{\bar{\phi}}$, $\bar{J}_\alpha$, $\bar{J}_\alpha^o$, $\bar{J}_\alpha^i$, $\bar{\phi}_\alpha$, and $\bar{M}_\alpha$. The nodal equations (2)-(4) are in general not satisfied by these quantities.

We introduce a set of "discontinuity factors" f_α, g_α^i, g_α^o and m_α such that the weighted quantities $(\bar{\phi}_\alpha / f_\alpha)$, $(\bar{J}_\alpha / g_\alpha^i)$, $(\bar{J}_\alpha^o / g_\alpha^o)$ and $(\bar{M}_\alpha / m_\alpha)$ obey Eqs. (1) to (5) when the reference eigenvalue, node-average fluxes and net currents are conserved.

These discontinuity factors are defined uniquely [Eq. (2) defines m_α, and Eq. (3) and its symmetric form for the opposite face define f_α and $f_{-\alpha}$ uniquely; g^o_α and g^i_α are then obtained from (4) and the relation between partial and net currents].

The mathematical expressions for calculating all discontinuity factors are given in Ref. 1.

N.E.T. was implemented in DIF3D nodal in a way that minimizes the loss of computational efficiency. Typical timing comparisons are given in Ref. 1, and indicate that only a slight loss of efficiency (less than 20%) is incurred for fast reactor problems.

6. APPLICATION OF NODAL EQUIVALENCE THEORY TO EBR-II CALCULATIONS

Modern three-dimensional transport codes either lack some features (such as hex-z geometry or, in the case of some transport codes, higher order scattering) or would be very slow running for realistic EBR-II calculations where large numbers of energy groups are required. Consequently, an alternative approach, which relies on N.E.T. has been developed. This approach relies on two basic observations:

- experience with performing EBR-II core neutronic calculations has shown that Radial-Z transport calculations using large numbers of energy groups lead to accurate predictions of the core global behavior when compared to higher order calculations or experimental results. In particular, these calculations yield acceptable estimates of the core eigenvalue and thus of the net leakage out of the core. Nevertheless, due to the cylindricization procedure involved in these calculations, they cannot accurately predict neutronic quantities in a specific assembly. Thus, calculations that represent the hexagonal planar layout of the core are needed.

- inspection of the formulas for the discontinuity factors in Ref.1 indicates that there is a partial decoupling between planar and axial discontinuity factors. In the expression for the planar discontinuity factors, the sole axial term is the node-averaged axial leakage; thus, it is expected that the planar discontinuity factors for a 3D model can be approximated from hexagonal 2D transport calculations, where the average axial leakage is introduced by means of an axial buckling or an appropriate neutron source. In a similar fashion the sole planar term in the mathematical expression for the axial discontinuity factors is the net planar leakage through the six faces of the hexagon. Thus, it is expected that the axial discontinuity factors can be approximated directly from the R-Z transport calculations.

A procedure has been developed for generation of the required discontinuity factors, and is now being automated. It consists of the following steps:

Step 1: the core geometry is cylindricized

Step 2: an Sn calculation is performed for that R-Z model, using a fine energy structure.

Step 3: the axial discontinuity factors are obtained directly from that calculation, and few-group cross-sections are obtained by a systematic condensation process, which relies on the fluxes computed in Step 2.

Step 4: the 2D discontinuity factors are obtained by adapting some ideas previously employed in 3D flux synthesis methods[12]:

- for planes within the active core, the axial bucklings can be directly computed from the R-Z calculation. A 2D Sn eigenvalue calculation is then performed, using these bucklings, and 2D discontinuity factors are obtained from the angular flux distribution.

- planes above or below the active core are highly sub-critical, as they contain little or no fissile material. The procedure used for planes within the active core would be inadequate, since some bucklings would have large negative values, and might prevent the Sn calculations from converging. Instead, a 2D fixed source calculation is run, where the source is set equal to the scattering integral of neutrons leaking from the core into the region of interest. This source is computed from the results of the R-Z calculation.

Step 5: the 2D and axial discontinuity factors are assembled and used in a 3D nodal run.

Three characteristics of the EBR-II core help to limit the number of 2D Sn calculations which are needed to analyze the core over its lifetime:

- the core cycle is quite short and the burnup over one cycle is small enough so that a unique set of discontinuity factors is sufficient through the cycle.

- the active core is quite homogeneous in the axial direction. A unique set of planar discontinuity factors can be used over its whole height

- loading modifications of the ex-core regions are infrequent. Thus, it is likely that planar discontinuity factors above and below the active core need to be recomputed only after several cycles.

A very simplified model of the EBR-II core was designed for validating this scheme (see Figures 2 and 3). Radially, the core comprised 7 rows of homogeneous binary fuel, surrounded by 4 rows of homogeneous radial reflector and 5 rows of homogeneous radial blanket. Above the core, the fission plenum, upper grid and upper axial reflector were represented as homogeneous regions. Below the core, the lower grid and lower axial reflector were represented as homogeneous regions. The radial reflector and the radial blanketwere taken to be homogeneous from the bottom to the top of the model.

The cross sections used for these compositions were from a typical 9 group set generated for the EBR-II core. It was assumed that the macroscopic cross sections remain constant through each of the eight regions defined in Figure 4. The energy condensation procedure described in Step 3 was not utilized.

For all transport calculations, neutron scattering was treated as isotropic (P0), with the standard transport correction applied to the total cross section and within-group scattering cross section

6.1 Reference Calculation

The reference calculation was obtained from the VIM Monte Carlo code[6], run in a multigroup mode, using the same set of 9-group cross sections. In order to obtain reasonable statistics (in particular for the radial blanket), 4,800,000 neutron histories were run.

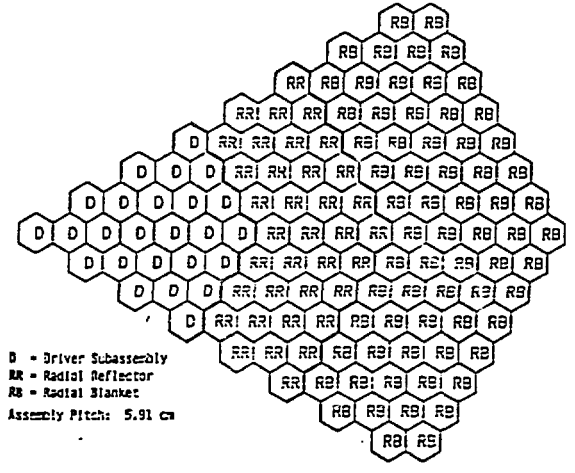

Figure 2: Planar Layout EBR-II Model

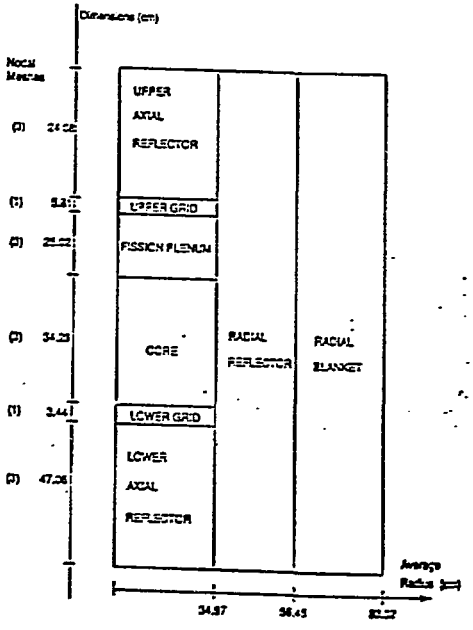

Figure 3: Axial Layout EBR-II Model

6.2 Computation of Approximate Discontinuity Factors

An R-Z model was set up, which cylindricizes the core by conserving the volume of each row of assemblies, and by exactly reproducing the axial dimensions.The mapping between R-Z and Hex-Z was obtained from the assumption that the quantities to be mapped (axial bucklings, scattering sources and axial discontinuity factors) are constant over each row.

The R-Z transport flux solution was obtained using TWODANT, with the S4 angular approximation and very fine radial and axial meshes. The angular fluxes were collapsed over the appropriate coarse meshes, in order to compute axial discontinuity factors for all rings.

The planar discontinuity factors were generated from S4 flux solutions obtained using DIF3D-Sn [13]with 6 triangles/hexagon. Four such calculations were performed:

- one eigenvalue calculation, at the core mid-plane, for a model comprising the full 16 rows, using axial bucklings constant over each row;
- three fixed source calculations (for the lower axial reflector, lower grid and fission plenum levels) for models comprising only the 10 innermost rows (thus reducing the computational cost by a factor of more than 2).

Axial discontinuity factors were mapped on the Hex-Z model by assuming they were constant over each row of assemblies.

6.3 Evaluation of Results

Results are compared to the reference VIM results for the R-Z Sn and diffusion runs, the standard nodal diffusion run with unity-valued discontinuity factors (UDF), and the nodal diffusion run with Approximate Discontinuity Factors (ADF).

TableIII compares the eigenvalues for all these runs. The error resulting from the use of ADF's is almost ten times smaller than the error resulting from the use of UDF's.

Figure4 compares the errors in axially and radialiy integrated in-situ powers computed by the different schemes. These powers represent the average value over each ring of the total in-situ power transmitted to the flowing sodium . Globally, the ADF scheme shows a very significant improvement over the standard UDF scheme. In particular, the power predictions in the radial reflector and blanket are significantly improved: for example, the maximum error in assembly power in the radial blanket is reduced from 4.7% to 1.2%. However, the standard diffusion theory solution accurately predicts the power distribution in the driver region.

Preliminary results indicate that the methodology described here is similarly successful when higher order scattering and energy condensation effects are taken into account.

TABLE III. EIGENVALUE COMPARISON FOR 3D EBR-II BENCHMARK

CASE	Keff	Error relative to VIM
VIM	1.20423+.00045	
R-Z dif	1.17603	-.02870
R-Z Sn	1.20991	+.00568
UDF	1.17691	-.02732
ADF	1.20711	+.00288

7. SUMMARY AND CONCLUSIONS

The need for accurate core depletion calculations in Experimental Breeder Reactor No. 2 (EBR-II) is discussed. Because of the unique physics characteristics of EBR-II it is difficult to obtain accurate and computationally efficient multigroup flux predictions. This paper describes the effect of various conventional and higher order schemes for group constant generation and for flux computations; results indicate that higher-order methods are required, particularly in the outer regions (i.e. the radial blanket). A methodology based on Nodal Equivalence Theory (N.E.T.) is developed which allows retention of the accuracy of a higher order solution with nearly the same computational efficiency of a few group nodal diffusion solution.The application of this methodology to three-dimensional EBR-II flux predictions is demonstrated; this improved methodology allows accurate core depletion calculations at reasonable cost.

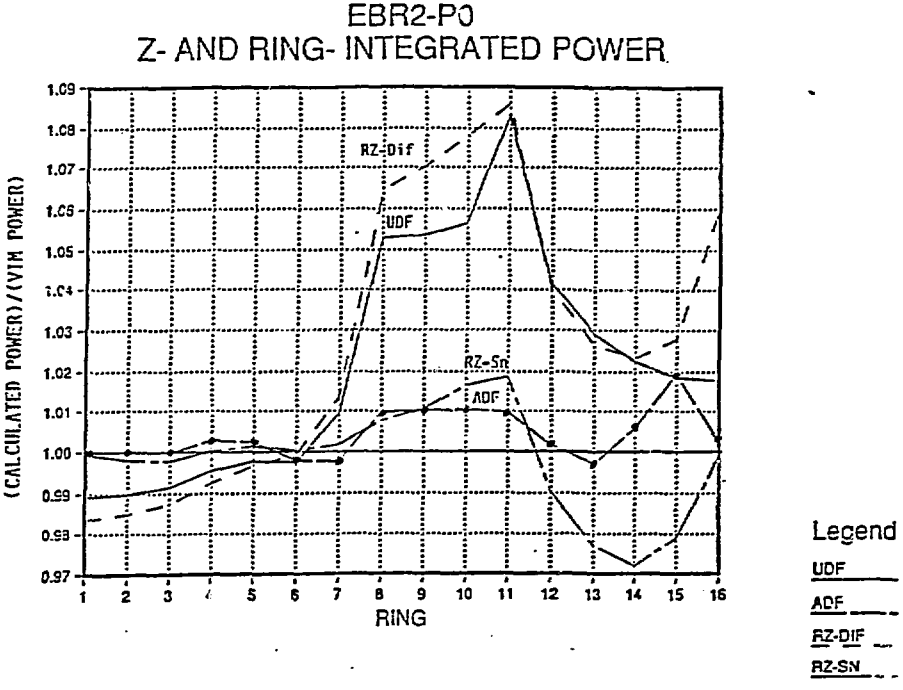

Figure 4: Axially Integrated Ring Power

8. REFERENCES

1. P.J. Finck and K.L. Derstine, "The Application of Nodal Equivalence Theory to Hexagonal Geometry Lattices," Proc. Intl. Topical Mtg. on Advances in Mathematics, Computations, and Reactor Physics, Pittsburgh, April 1991

2. R.N. Hill and K.O. Ott, "Advanced Methods Comparisons of Reaction rates in the Purdue Fast Breeder Blanket Facility," Nuclear Science and Engineering, 103, 12 (1989)

3. R.N. Hil, K.O. Ott and J.D. Rhodes,, "Directional Effects in Transitional Resonance Spectra and Group Constants," Nuclear Science and Engineering, 103,25 (1989)

4. H. Henryson II, B.J. Toppel, and C.G. Stenberg, "MC2-2: A Code to Calculate Fast Neutron Spectra and Multigroup Cross Sections, " ANL-8144, Argonne National Laboratory (June 1976)

5. R. E. Alcouffe et al., "User's Guide for Twodant: A Code Package for Two-Dimensional, diffusion Accelerated, Neutral-Particle, Transport," LA-10049-M, Los Alamos National Laboratory (1988).

6. R. N. Blomquist, "VIM Users Guide," Argonne National Laboratory, 1987.

7. K.L. Derstine, "DIF3D: A Code to Solve One-, Two-, and Three-Dimensional Diffusion Theory Calculations in Hexagonal Geometry,"ANL-82-64, Argonne National Laboratory (1984)

8. K.S. Smith, "Assembly Homgenization Techniques for Light Water Reactor Analysis," Prog. Nucl. Energy, 17, 3, 305 (1986).

9. K. S. Smith, "QPANDA: An Advanced Nodal Method for LWR Analysis," Trans. Am. Nucl. Soc., 50, 532 (1985).

10. M.H. Chang, "The Application of Nodal Methods to the Transport Equation",Ph.D Dissertation, Department of Nuclear Engineering, MIT, Cambridge, MA (1984).

11. R. D. Lawrence, "The DIF3D Nodal Neutronics Option for Two- and Three-Dimensional Diffusion Theory Calculations in Hexagonal Geometry, ANL-83-1, Argonne National Laboratory (1983).

12. .C. H. Adams, ANL, private communication (1989).

13. E.E. Lewis, "The DIF3D Transport Extension for Discrete Ordinate Neutronics Calculations in Two Dimensions," FRA-TM-149, Argonne National Laboratory (1983).